UV Polymerization of Oligothiophenes and Their Application in Nanostructured Heterojunction Solar Cells

Carolien L. Huisman,*,† Annemarie Huijser, Harry Donker, Joop Schoonman, and Albert Goossens

Laboratory for Inorganic Chemistry, Faculty of Applied Sciences, Delft University of Technology, Julianalaan 136, 2628 BL, Delft, The Netherlands

Received November 17, 2003; Revised Manuscript Received May 5, 2004

ABSTRACT: Thin films of 2,2′-bithiophene (2T) and 2,2′-5′,2″-terthiophene (3T) are polymerized by UV irradiation. The polymerization process can be observed by UV−vis and photoluminescence spectroscopy. If 2T is used as starting material, predominantly 4T (quarterthiophene) is formed, while 6T (sexithiophene) is formed if 3T is used as starting material. The same polymerization reaction occurs if solutions of 2T or 3T in chloroform or toluene are used or if a film of nanocrystalline titanium dioxide (nc-TiO_2) is soaked with a 2T or a 3T solution. In the latter case the pores are (partly) filled with 4T or 6T, which acts as hole conductor. A photovoltaic response is observed when nc-TiO_2/4T or nc-TiO_2/6T interpenetrating structures are irradiated with visible light. The increase of oligomer length from 2T to 3T and the corresponding decrease in orientational freedom of the molecules strongly affects the ease of polymerization and the structural order of the compounds formed.

Introduction

Conjugated oligomers and polymers of thiophenes have found application in various optical and electrical devices, like electrochromic windows and organic thin-film transistors. Unsubstituted, unbranched oligothiophenes are abbreviated by α-*n*T, in which *n* stands for the number of repeating units. α indicates the positions of the thiophene ring where they are linked together (see Figure 1B).

Because of π-stacking in the solid state, hole mobilities for the higher oligomers and polymers can reach a few 10^{-2} cm^2 V^{-1} s^{-1}.[1] The electronic structure of oligothiophenes largely depends on the number of repeating units. As the HOMO−LUMO gap decreases for increasing *n*, the absorption and luminescence peaks shift to the red. Also, the oxidation potential and the energy of the excited states are influenced. The fluorescence quantum yield of α-4T is around 2×10^{-2}, but for α-5T to α-8T this yield is much lower ($\leq 10^{-3}$), while it decreases further for more ordered films. In Table 1 literature values for absorption and luminescence maxima of oligothiophenes are presented.

Hybrid solar cells (also referred to as organic solar cells) have been developed in the past decade as an alternative for silicon-based solar cells. A wide band gap metal oxide, like TiO_2, is sensitized by a visible light-absorbing species that can be inorganic or organic in nature. Other combinations of materials are also possible. A laminar device structure has shown to yield cells with limited efficiency (<1%) due to the limited interfacial area. Extensive recombination occurs, as the exciton diffusion length in most organic semiconductors is only a few nanometers. Enlargement of the interfacial area is accomplished in dye-sensitized solar cells, in which a highly porous film of titanium dioxide nanoparticles is covered with a monolayer of a metal−organic sensitizer that absorbs visible light. Although to date the energy conversion efficiency exceeds 10%,[16,17] the necessity of a liquid electrolyte to accomplish regeneration of the oxidized dye calls for elaborate sealing techniques, which has hindered commercialization thus far. One especially interesting approach to eliminate the need for a liquid electrolyte inside the device is the use of solid organic or inorganic hole conductors. These compounds can function as light-absorbing species and inject electrons into the conduction band of the n-type semiconductor, while, at the same time, they conduct the holes to the back contact. For inorganic compounds this concept has been successfully proven in the extremely thin absorber (ETA) TiO_2/$CuInS_2$ solar cell.[18−23] For organic systems, blends of PPV and C60 derivatives are intensively studied and show an efficiency of 3% under simulated solar light.[24−26] Oligo- and polythiophenes have been studied for incorporation into hybrid solar cells, where they act as visible light absorbers and electron donors in combination with, for example, metal oxide or fullerene electron acceptors. Recently, a bulk heterojunction of CdSe nanorods and poly(3-hexylthiophene) has been developed with an efficiency of 1.7% under AM 1.5 conditions.[27] In solar

Table 1. Absorption and Fluorescence Peaks for Solutions and Thin Films of Oligothiophenes (α-*n*T)[a]

	absorption		fluorescence	
	solution (nm)[b]	film (nm)	solution (nm)[b]	film (nm)
α-2T	302		362	380
α-3T	355		407, 426	
α-4T	390	448	437, 478	532, 579
α-5T	416	488	482, 514	554, 592
α-6T	432	513	510, 542	588, 640
polythiophene		486		620, 689

[a] All values are taken from *The Handbook of Oligo- and Polythiophenes*,[1] but similar values have been found in other articles.[2−15] [b] Measured in chloroform. In other reports EPA, dichloromethane, and dioxane/acetronitrile are used as solvent, showing no apparent differences for the peak positions.

† Current address: Solid State Chemistry, Institute for Physics, University Augsburg, Universitätsstrasse 1, D-86159 Augsburg, Germany.

* Corresponding author: e-mail Caroline.Huisman@physik.uni-augsburg.de.

10.1021/ma0357265 CCC: $27.50
Published on Web 06/29/2004

cells a large overlap between the absorption spectrum of the active material and the solar spectrum is desired. Hence, the higher oligomers are more suited for this purpose. Sexithiophene is regarded to exhibit already most of the properties of polythiophene because shifts in absorption and hole mobility as a function of n are leveling off for higher oligomers. Adding alkyl chains to the thiophene backbone induces peak shifts, in most cases to the red, as a result of less π-overlap between adjacent chains.[1] End substitution or addition of long alkyl chains (more than six carbon atoms) to the backbone, on the other hand, leads to better orientation[1,28] and to higher hole mobilities.

To synthesize a similar system based on nc-TiO_2, several challenges are encountered. First of all, the pores of the system should be rather small in order to prevent extensive bulk recombination inside the organic phase. However, for smaller pore sizes it becomes increasingly more difficult to fill them with bulky dyes. Recently, we have investigated the penetration depth of poly(3-octyl)thiophene (P3OT) inside nanoporous TiO_2 and observed this depth to be limited to about 1 μm for an average particle size of 50 nm. For TiO_2 particles of about 9 nm the maximum penetration depth of P3OT is less than 300 nm.[29] Because a high-temperature step is necessary to obtain good-quality anatase TiO_2 and most organic materials are not stable at these high temperatures, premixing with TiO_2 particles is not possible. Recently, a nanostructured heterojunction of MDMO−PPV and TiO_2 was investigated, in which amorphous TiO_2 was formed from a precursor in the presence of the polymer.[30] MEH−PPV was spin-coated onto nanoporous TiO_2, but the PV effect was limited.[31] It was shown to be possible to infiltrate poly(3-hexylthiophene) into nanoporous TiO_2 by a melting technique.[32] Yet another approach is to infiltrate the TiO_2 pores with small organic molecules from solution, which will have a larger penetration depth compared to large oligomers or polymers. For oligothiophenes, however, only the smallest oligomers are soluble, which merely absorb in the ultraviolet part of the solar spectrum. From literature, it is known that oligothiophenes can be polymerized wet−chemically (using, for example, $FeCl_3$)[33−40] as well as electrochemically.[41,42] Both methods are not or hardly suitable for in-situ polymerization in a nanoporous system because of size constraints. There are indications that polymerization of thiophene and bithiophene films can be induced by electron beam or X-ray irradiation.[43−45] Photochemical polymerization of oligothiophenes has not been reported in great detail, but some studies indicate that small oligomers are formed.[46,47]

This paper presents an investigation of the photochemical polymerization of 2,2′-bithiophene (α-2T) and 2,2′-5′,2″-terthiophene (α-3T) thin films using UV irradiation. The polymerization reaction is monitored by UV−vis absorption and fluorescence spectroscopy. Evidence is shown for the occurrence of a dimerization reaction that transforms 2T into 4T and 3T into 6T. This transformation can be established in thin films, in solutions, and inside nanoporous TiO_2. The peak positions in the absorption and photoluminescence (PL) spectra indicate that a nonordered structure is formed for the thin films, which can be crystallized at higher temperatures for 2T → 4T films. In nc-TiO_2 the absorption and PL peaks of 2T before and after irradiation are at higher wavelengths, indicating that a more ordered structure is formed. The orientational freedom for 2T molecules is larger than for 3T molecules, leading to more facile polymerization and the formation of more ordered structures. We will also describe that filling of a nanoporous TiO_2 film with 2T or 3T solutions yields, after UV irradiation, cells that clearly show a photovoltaic effect.

Experimental Section

2,2′-Bithiophene (97%) and 2,2′-5′,2″-terthiophene (99%) are obtained from Aldrich and are used without further purification. Solutions of either 1 or 40 mg/mL are prepared in chloroform (Aldrich, anhydrous 99+%). Thin films are prepared by spin-coating; first, 5 drops of a 40 mg/mL solution of 2T or 3T are applied on a substrate, which is subsequently rotated at 1500 rpm for 20 s. The films are immediately used for experiments to prevent evaporation of the volatile 2T and 3T. The film thickness of the 2T/3T films is estimated to be around 300 nm.

For the optical measurements quartz substrates (1 × 1 in., ESCO) are used. Quartz does not show any absorption for wavelengths above 250 nm. As substrate material for the photovoltaic measurements, fluorine-doped SnO_2 is used (Transparent Conducting Oxide, Libbey Owens Ford, 20 Ω cm^2). Substrates are thoroughly cleaned in an ultrasonic bath with ethanol and acetone successively and then dried in a dry nitrogen stream. The TCO is covered with a thin dense film of anatase TiO_2 (70 nm), deposited by spray pyrolysis,[48] and subsequently a nanoporous TiO_2 film is deposited on top by doctor blading of a paste of 15 nm TiO_2 particles (Solaronix T, BN 91/21051T). The nc-TiO_2 film is annealed at 450 °C for 2 h, yielding an 8−10 μm thick electron-conducting network. For several experiments the nc-TiO_2 particles are covered with a monolayer of ruthenium dye (Ru535, *cis*-[$L_2Ru(SCN)_2$] in which L stands for 2,2′-dipyridine-4,4′-dicarboxylic acid, Solaronix BN 119,0898, 0.3 mM in ethanol).

For comparison with the polymerized 3T, a fluorescence spectrum is recorded for a 120 nm thin film of 6T, deposited using a thermal evaporation setup with a rate of 2 nm/s. The 6T is purchased from Syncom and is purified by zone sublimation.

UV−vis absorbance spectra are recorded on a Varian Cary 1 UV−vis spectrophotometer. Thin films of 2T and 3T on quartz as well as inside nanoporous TiO_2 are measured before and after different times of UV irradiation. A similar experiment is performed with quartz cuvettes containing solutions of 2T and 3T in chloroform.

For UV irradiation of the samples a 150 W water-cooled xenon lamp is used, which emits light in the region between 250 and 1100 nm. Because the heat dissipated by the lamp evaporates the oligothiophene films from the quartz substrates, the samples are cooled by placing them on a "cold-finger", cooled with liquid nitrogen. The distance from lamp to sample is kept constant at 15 cm, and the intensity on the sample is approximately 3 W/cm^2.

Photoluminescence spectra are recorded with a home-built setup, using the third harmonic of a pulsed Nd:YAG laser (355 nm, 10 Hz) as excitation source. An intensity of 0.25 mW per pulse and a pulse length of a few nanoseconds are used (intensity on sample approximately 0.5 mW/cm^2 per pulse). Fluorescence is recorded in a 90° geometry for quartz substrates and cuvettes, using two high pass filters of 380 nm to remove the laser light. Spectra are recorded using a liquid nitrogen cooled CCD camera (Princeton Instruments LN/CCD-1100PB) and a Spex 340E monochromator equipped with a 100 grooves/mm grating, blazed at 500 nm. For low-temperature measurements a closed-cycle helium cryostat is used. In-situ measurements are performed on the polymerization of pristine 2T or 3T thin films on quartz or inside nc-TiO_2 and in 2T/3T solutions in quartz cuvettes by the UV light of the pulsed laser, while changes in the PL spectra are recorded simultanously. No corrections for the filters and the sensitivity of the CCD camera and the monochromator are applied.

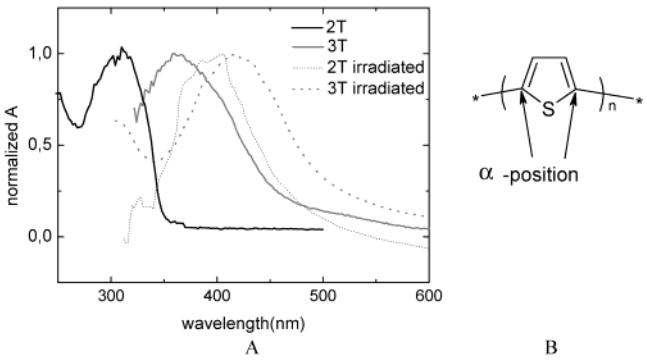

Figure 1. (A) Absorbance of thin films before and after 10 min of UV irradiation. Illuminated spectra are corrected for presence of starting material, and all spectra are normalized. (B) Structure of α-*n*T.

Current−voltage characteristics and wavelength-dependent photocurrent spectra are recorded using a Keithley 2400 source meter. A 250 W tungsten−halogen lamp in combination with an Acton Spectra-Pro-275 monochromator is used to illuminate the samples through the TCO substrate with an intensity of 100 mW/cm^2 in the case of white light and with ca. 2 mW/cm^2 in the case of monochromatic light. The light source is not AM 1.5 calibrated. A 360 nm high-pass filter is used to measure the wavelength-dependent photocurrent spectra. Evaporated gold contacts with a diameter of 2 mm and a thickness of 50 nm are used as back contacts. Contact to the gold is made with a gold-coated tip, attached to a spring with a spring constant of 7×10^{-3} N m^{-1} (Ingun Prüfmittelbau GmbH). Some measurements are carried out using mercury contacts, yielding the same results as for gold contacts. Measurements are performed at ambient conditions. Care is taken to keep the samples in the dark as much as possible to avoid exposure to light, as this is known to cause degradation of semiconducting polymers.[1,49] To lower the resistance of the cells, a film of PEDOT:PSS (poly(3,4-ethylenedioxythiophene:poly(styrenesulfonate) (Bayer AG, Baytron P) is spin-coated on top of the TiO_2/oligothiophenes blend. PEDOT-PSS is a highly doped p-type material, selectively conducting holes.[50] First the sample is moistened with a few drops of acetonitrile (Aldrich, p.a.) to increase the wettability of the surface. A solution of PEDOT:PSS in water, containing about 5 vol % of acetonitrile, is spin-coated on the sample, yielding a thin film of about 50 nm.

Results and Discussion

UV Irradiation of 2T and 3T Thin Films: Absorbance Spectra. 2,2′-Bithiophene and 2,2′-5′,2″-terthiophene are transparent crystals and light yellow powders, respectively, that easily dissolve in polar solvents like chloroform, toluene, water, and acetone. During UV irradiation, thin films or solutions of 2T and 3T turn orange/brown. For solutions it is observed that in time the reaction products precipitate.

In Figure 1, the absorbance spectra of thin films of 2T and 3T on quartz before and after 10 min of UV irradiation are shown. In the spectra of the irradiated 2T/3T samples a new peak, about 80 nm shifted to the red, is clearly visible. For clarity, the spectrum of the sample before irradiation is subtracted, as starting material is still present. As mentioned above, the absorption peak of α-*n*T shifts to the red with increasing oligomer length. As a result of the UV irradiation, the 2T and 3T are (partly) transformed into higher oligomers. To which extent the oligomers are polymerized will be discussed in the next section.

UV Irradiation of 2T and 3T Solutions: Absorbance Spectra. Figure 2 shows absorbance spectra for

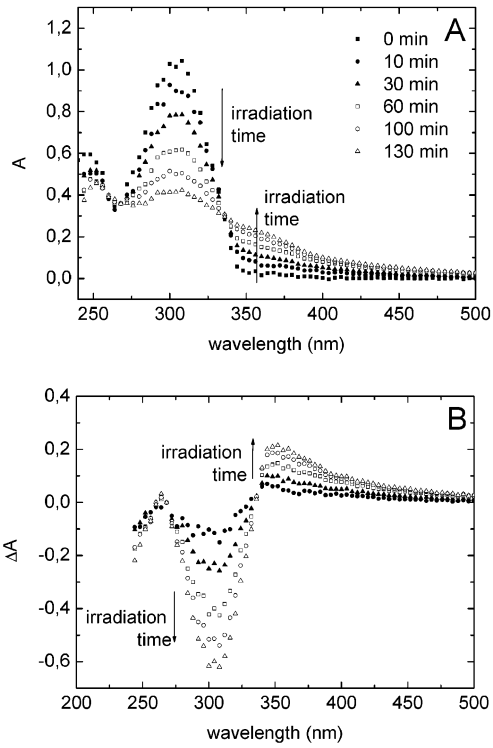

Figure 2. (A) Absorbance of 2T in chloroform before and after different times of UV irradiation. (B) Difference spectra between irradiated and pristine (nonirradiated) solution. The concentration of the illuminated solution is 1 mg/mL, which is diluted to 0.01 mg/mL for the measurements.

2T in chloroform (1 mg/mL) before and after different UV irradiation times. Also, the difference spectra before and after irradiation are shown. It is clearly visible that a new peak appears, shifted about 60 nm to the red as a result of the irradiation. An isosbestic point is observed, indicating a complete transformation from one starting material to one product.

In Figure 3, the same experiment is shown for 3T in chloroform. Again, a new peak appears, shifted approximately 80 nm to higher wavelengths. Also here, an isosbestic point is observed.

Comparing the peak data with the literature values in Table 1, it is clear that 2T is transformed into 4T and 3T into 6T. A polymerization reaction is taking place, induced by the UV irradiation. For thin films on quartz, the absorption peak values are similar to those of solutions. This indicates that a nonordered structure is formed since normally films have an absorption that is more red-shifted (see Table 1).

UV Irradiation of 2T and 3T Thin Films: Photoluminescence Spectra. To investigate the polymerization reaction in detail, photoluminescence (PL) experiments are performed. In Figure 4, the PL spectra are shown for thin films of commercially obtained 2T, 3T, and 6T. Although literature data for 3T films are not available, the peak positions of 2T and 6T are in agreement with the literature (see Table 1).

Figure 5 shows an in-situ experiment, in which a freshly deposited film of 2T on quartz is continuously irradiated with 355 nm laser pulses, while the PL spectrum is measured every 2 s. Clearly a transformation in the spectra is observed as a result of the irradiation, and the peak positions shift about 80 nm to the red. An isosbestic point is observed, indicating that the transformation is complete, and one reaction

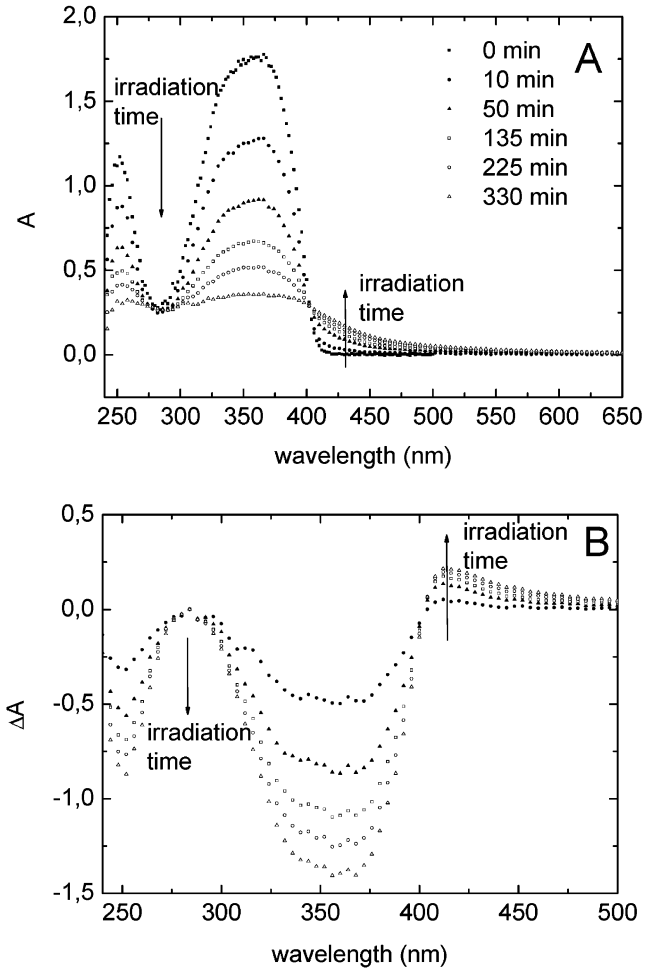

Figure 3. (A) Absorbance of 3T in chloroform (1 mg/mL) before and after different times of UV irradiation. (B) Difference spectra between irradiated and pristine solution. The concentration of the illuminated solution is 1 mg/mL, which is diluted to 0.01 mg/mL for the measurements.

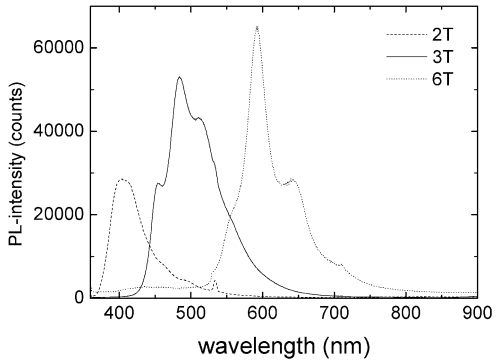

Figure 4. PL spectra of 2T, 3T, and 6T thin films on quartz, measured at ambient pressure and temperature. Laser excitation is performed at 355 nm and 10 Hz, with a pulse length of a few nanoseconds and an intensity of 0.25 mW per pulse.

product is formed. After about 250 s, the intensity of the spectra decreases over the whole wavelength range, and no intersection with the isosbestic point is present anymore. It can be concluded that a decomposition or evaporation process occurs, leaving less luminescent material on the substrate.

In Figure 6, the same experiment is shown for 2T inside a porous nc-TiO_2 film. Again a clear transformation is observed, exhibiting an isosbestic point. The peak positions are at higher wavelengths than for a thin 2T

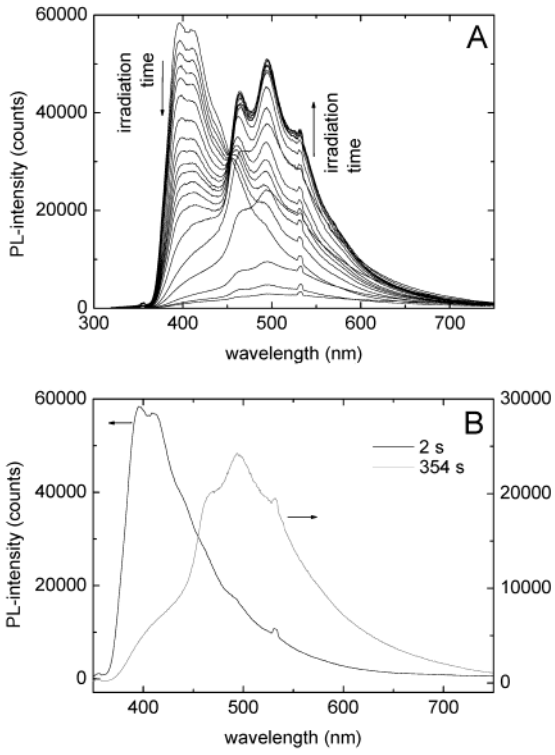

Figure 5. In-situ polymerization of a 2T thin film on quartz at ambient pressure and temperature. (A) PL spectra are taken at 2, 4, 6, 8, 10, 14, 24, 34, 44, 54, 64, 74, 84, 104, 154, 254, 354, 554, 754, and 1015 s after the start of the irradiation. (B) PL spectrum at $t = 2$ s and at $t = 354$ s.

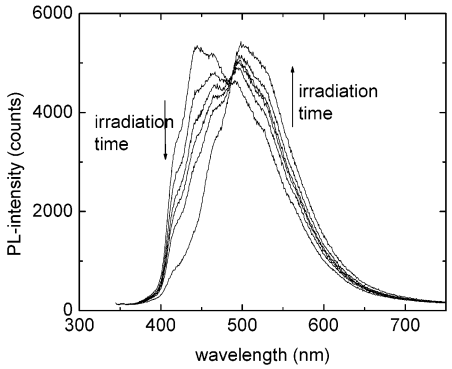

Figure 6. PL spectra of a thin film of 2T inside nc-TiO_2 at ambient pressure and temperature. PL spectra are taken at 90, 150, 210, 270, 360, and 900 s after the start of the irradiation.

film on quartz, indicating a higher ordering inside nc-TiO_2.

The same experiment is repeated with thin films of 3T on quartz, but no change in spectra is observed, except for a continuous decay in time over the full wavelength range. Afterward, no film is present on the substrate, indicating that evaporation occurrs during irradiation. This experiment is repeated at 6 K under vacuum, but again evaporation occurs. Lowering the intensity of the laser to 0.2 mW/pulse or less prevents evaporation, but the PL spectra remain unchanged in time, indicating that no polymerization reaction is induced at lower energies.

UV Irradiation of 2T and 3T inside nc-TiO_2: Absorbance Spectra. The experiment is repeated at room temperature with a nanoporous film of TiO_2 soaked with 3T. In this case a change in spectra is

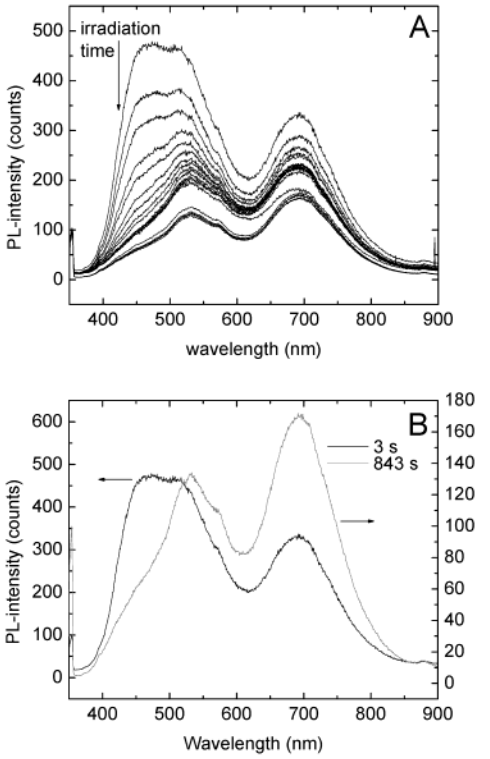

Figure 7. PL spectra of a thin film of 3T inside nc-TiO_2 at ambient pressure and temperature. (A) PL spectra are taken at 33, 36, 39, 51, 60, 90, 120, 180, 240, 300, 450, 510, 570, 600, 615, 645, 675, 765, and 843 s after the start of the irradiation. (B) PL spectrum at $t = 3$ s and at $t = 843$ s.

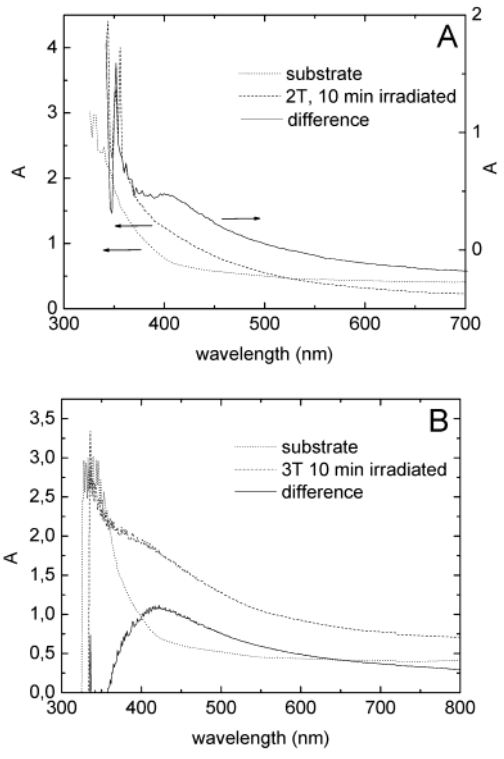

Figure 8. Absorbance spectra of 2T (A) and 3T (B) inside nanoporous TiO_2, after 10 min of irradiation at ambient pressure and temperature at 355 nm, with a pulse length of a few nanoseconds, a pulse frequency of 10 Hz, and an intensity of 0.25 mW per pulse. Spectra of the substrate: TCO/TiO_2/nc-TiO_2, the substrate with 2T (A) or 3T (B) after irradiation, and the difference spectrum of sample and substrate are shown.

observed during laser irradiation (Figure 7), but no isosbestic point is present. This indicates that some evaporation still takes place during irradiation. After the experiment, an orange-brown spot is observed on the sample. In Figure 8A, the absorbance spectra of the colored region and the substrate (TCO/TiO_2/nc-TiO_2) as well as the difference between the two are plotted. A peak appears, which is at the same position as the peak of irradiated 3T on quartz in the absorbance spectra shown in Figure 1. Hence, it is concluded that indeed the same reaction has occurred in the laser experiment as during UV irradiation using the xenon lamp. In Figure 8B, the same absorbance spectra for 2T/nc-TiO_2 after the in-situ PL experiment are shown. It is visible in Figure 8 that the absorbance does not go to zero at long wavelengths. This is a result of light scattering on the samples.

UV Irradiation of 2T and 3T Solutions: Photoluminescence Spectra. In-situ PL experiments are also performed on solutions of 2T and 3T. Because chloroform is a strong luminescent solvent, toluene is chosen instead. In Figure 9, PL spectra are shown for a 1 mg/mL solution of 2T in toluene, measured as a function of irradiation time. As can be seen from the difference spectrum before and after irradiation a new peak appears, shifted 90 nm to the red. For the same experiment with 3T in toluene no new peaks occur during irradiation, but only a decrease in intensity is observed over the full wavelength range (not shown). After the experiment, the 3T/toluene solution was colored orange/brown. Tentatively, the absence of a clear transformation in the PL spectra is ascribed to the formation of a compound, which shows only limited or even no luminescence. From the literature it is known that the fluorescence quantum yield of 6T is lower than of 4T (see Introduction), so it may very well be also lower than of 3T. This could lead to a situation where the formation of 6T is not seen in the PL spectrum.

Heat Treatment of Polymerized 2T and 3T Thin Films: Absorbance Spectra. In Figure 10, absorbance spectra of 2T on quartz are shown, before and after 45 min of UV irradiation and after subsequent annealing at 100−300 °C. From the difference spectra (Figure 10B), it can be seen that at a temperature of 200 °C the absorption peak shifts about 45 nm to the red. Higher temperatures do not induce a further change, and at 300 °C a decrease of the absorbance over the full wavelength range is observed, indicating that a decomposition or evaporation reaction is taking place. For 3T, either on quartz or inside nc-TiO_2, no peak shift in the absorbance spectrum is observed if a comparable annealing experiment is performed.

Absorbance and Photoluminescence Peak Positions. In Table 2, the measured peak values for all absorbance and PL spectra are summarized. A comparison of these values with those from literature (Table 1) reveals differences. While the experimentally obtained peak positions for the solutions are comparable to the literature data, the experimentally obtained peak positions for the thin films are close to the solution values. Furthermore, for the reaction of 2T to 4T inside nc-TiO_2, the experimentally obtained peak positions are in between the literature data for solutions and films, while for the reaction of 3T to 6T inside nc-TiO_2 the experimentally obtained peak positions are comparable to the literature solution values.

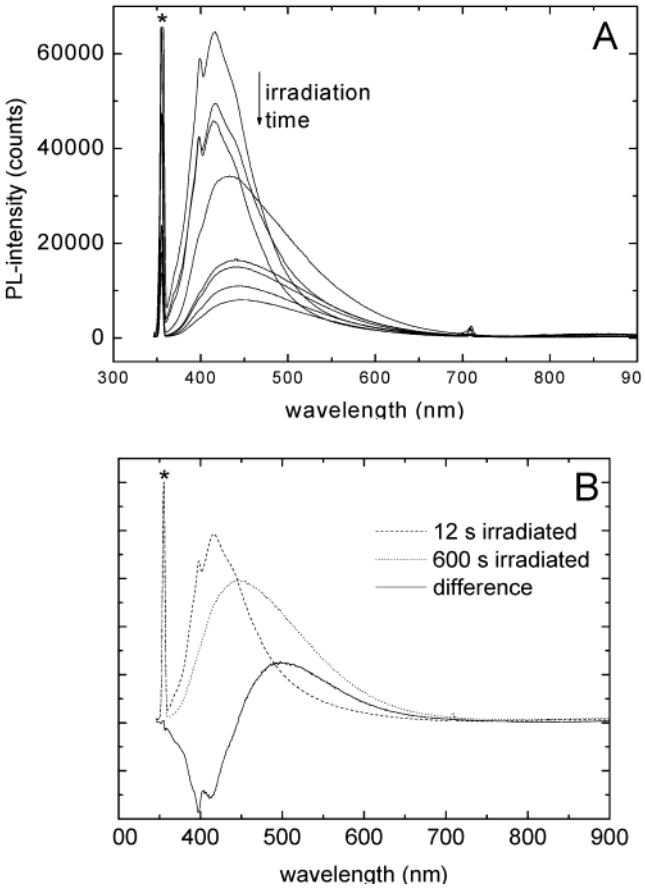

Figure 9. PL of 1 mg/mL 2T in toluene at ambient pressure and temperature. (A) PL spectra are taken at 12, 20, 160, 200, 300, 400, 500, and 600 s after the start of the irradiation. The asterisk denotes the excitation wavelength (355 nm). (B) PL spectrum at $t = 12$ s, normalized by taking the intensity at 355 nm as 100, normalized PL spectrum at $t = 600$ s, and difference spectrum of normalized spectra at $t = 600$ s and $t = 12$ s.

From literature it is known that the α-position of the thiophene ring is most reactive. Polymerization takes place through the formation of radicals. In this system two oligothiophene units are coupling, indicating that two radicals react with each other. This explains that polymerization is only observed if a high light intensity is applied, as a high concentration of radicals is necessary for this coupling to occur. In the photoluminescence experiments, it is observed that a light intensity beyond a certain threshold is required in order to start the polymerization reaction. Longer oligomers have less orientational freedom, explaining the inhibited transformation of 3T to 6T as compared to 2T to 4T. In nc-TiO_2 more oligomer molecules are present, which also have a higher orientational freedom. This could explain that 3T inside nc-TiO_2 is more easily polymerized. The experimentally obtained peak positions for the reaction of 2T to 4T inside nc-TiO_2 are in between the literature data for solutions and films, while for the reaction of 3T to 6T inside nc-TiO_2 the experimentally obtained peak positions are comparable to the solution values. This indicates that a more ordered structure is formed inside nc-TiO_2 for 2T as compared to 3T. This effect may also be related to the size and corresponding freedom of the oligomers during the polymerization reaction. After the light-induced polymerization of 2T the peak position is shifted to the literature values for thin films, if a temperature of 200 °C is applied (see Figure 10).

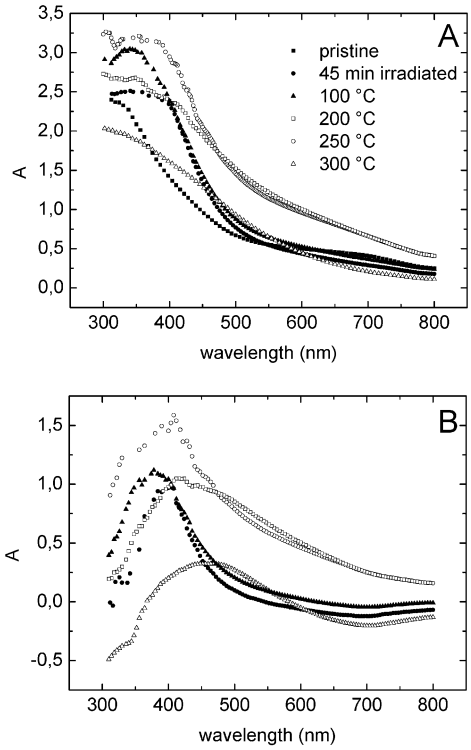

Figure 10. Absorbance spectra of an irradiated 2T film on quartz during annealing. (A) Before (■) and after 45 min (●) of UV irradiation and after subsequent heating at 100 °C for 2 h (▲), at 200 °C for 2 h (□), at 250 °C for 2 h (○), and at 300 °C for 2 h (△). (B) Difference spectra between the absorbance spectra after the heating steps and before UV irradiation and annealing.

The structural order is increased, while for 3T at elevated temperatures such an increase is not observed, showing once more that structural changes involving molecular reorientations are inhibited for longer oligomers.

UV Irradiation of 2T and 3T inside nc-TiO_2: Solar Cells. Nanoporous TiO_2 films are soaked with 2T or 3T solutions (40 mg/mL in chloroform) and are subsequently irradiated with a xenon lamp. $I-V$ curves and wavelength-dependent photocurrent spectra are recorded afterward. Layer thicknesses, particle sizes, and irradiation times are varied to investigate the photovoltaic characteristics of the cells. Cells that consist of TCO/TiO_2/nc-TiO_2/(2T or 3T)/Au exhibit a high resistance and low currents both in the dark and under irradiation. Applying a thin film of PEDOT:PSS improves the hole transport and yields a good diodic behavior in the dark and a photovoltaic effect under irradiation. In Figure 11A, $I-V$ curves are shown for a system with irradiated 3T inside the TiO_2 pores and for a system in which the nc-TiO_2 is first sensitized using a ruthenium dye, after which the sample is soaked in a 3T solution and irradiated. If the ruthenium dye is present, the short-circuit current is increased by a factor of 5 and the open-circuit voltage is also slightly higher. In Figure 11B, wavelength-dependent photocurrent spectra are presented for these cells, corrected for the lamp spectrum. If ruthenium dye is added, the photocurrent increases substantially. Therefore, light absorption, exciton transport toward the TiO_2, and electron injection of the oligothiophene are possible bottlenecks for the cells without Ru dye. The overall PV effect, if ruthenium dye is present, could be limited by various

Table 2. Experimentally Obtained Values for Absorbance and Fluorescence Maxima for Oligothiophenes (*n*T) in Solution, in Thin Films, and inside nc-TiO_2[a]

	absorption			fluorescence		
	solution (nm)	film (nm)	nc-TiO_2 (nm)	solution (nm)	film (nm)	nc-TiO_2 (nm)
2T	328	310		398, 410	396, 410	419, 442
3T	343	364		411, 434	483, 513	470, 508
4T	352	392	404	502	465, 494	499, 521
6T	416	418	423			530, 569

[a] 2T and 3T are starting materials; 4T and 6T are formed by UV-induced polymerization.

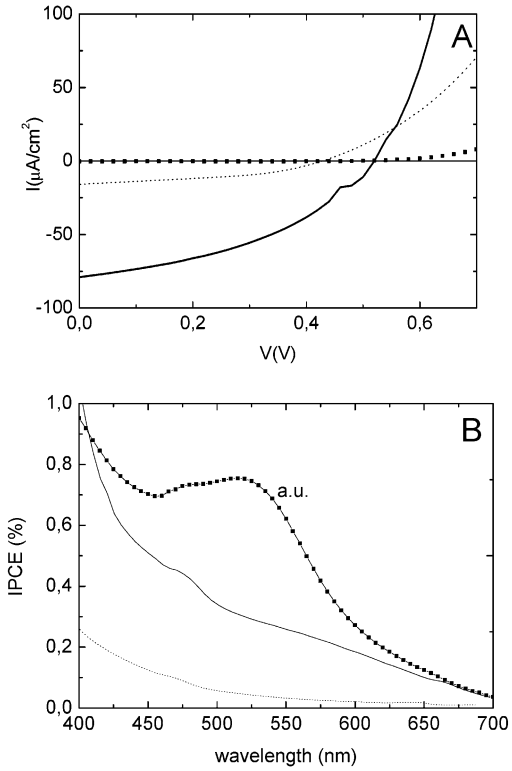

Figure 11. (A) *I*−*V* spectra of TCO/TiO_2/nc-TiO_2 + 3T/PEDOT:PSS/Au in dark (squares) and under white light irradiation (1000 W/m²) (dotted line) and of TCO/TiO_2/nc-TiO_2 + Ru + 3T/PEDOT:PSS/Au under white light irradiation (1000 W/m²) (solid line). (B) Incident photon to current efficiency (IPCE) curves of TCO/TiO_2/nc-TiO_2 + 3T/PEDOT:PSS/Au) (dotted line) and TCO/TiO_2/nc-TiO_2 + Ru + 3T/PEDOT:PSS/Au (solid line). The squares represent the IPCE curve of a typical dye-sensitized solar cell (TCO/nc-TiO_2 + Ru/I_2, I^-/TCO) in arbitrary units.

reasons, including incomplete filling of the pores of the nc-TiO_2 and low electronic conductivity inside the oligothiophenes (and, hence, ohmic losses). It is interesting to compare the spectrum of the Ru dye cell with a "standard" dye-sensitized solar cell (see Figure 11B). It is clear that the peak around 425 nm stems from the Ru dye, but this dye normally absorbs maximally at 520 nm. At this wavelength, however, not much activity is observed in the case of the UV-irradiated 3T cell. The reason for this deviation of absorption and photocurrent action spectra is not understood until now. For 2T inside nc-TiO_2 a more ordered structure is formed compared to 3T. Nevertheless, the solar cells characteristics of 3T/TiO_2 are better. This is probably due to the improved light absorption of 6T compared to 4T. A higher ordering of the materials is expected to a higher mobility, less resistance, and a longer exciton diffusion length, but because no optimization is performed, this effect can be canceled out for example by poor pore filling. More research is needed to clarify these issues.

Conclusions

High-intensity UV irradiation is capable of polymerizing bithiophene (2T) and terthiophene (3T). Radicals of these oligothiophenes, formed as a result of the irradiation, merge, forming an oligomer twice as long as the starting compound. This polymerization reaction can be observed using UV−vis absorbance and fluorescence spectroscopy. The systems investigated include solutions, thin films on quartz, and oligothiophenes inside nanoporous TiO_2. It is concluded that the increase of oligomer length from 2T to 3T and the corresponding decrease in orientational freedom of the molecules has a negative effect on the ease of polymerization and the structural order of the product. For 2T a thin film on quartz is transformed into an amorphous 4T film, while the same reaction occurring inside nc-TiO_2 yields a more ordered structure. Elevated temperatures lead to crystalline layers. For 3T nonordered structures are formed both for thin films on quartz and inside nc-TiO_2, while no evidence is found for ordering at higher temperatures. Furthermore, the fluorescence intensity during the reaction of 3T to 6T is decreasing (for nc-TiO_2) or disappearing (for toluene solutions) in time, while for the reaction of 2T to 4T a clear isosbestic point is observed, indicating that the former reaction is indeed inhibited compared to the latter. For polymerized 2T and 3T inside nc-TiO_2 a photovoltaic effect is observed. The reason for the limited photocurrent in this system requires more research. However, it is shown that an interpenetrating network of nc-TiO_2 and oligothiophenes can indeed be formed using in-situ UV polymerization.

References and Notes

(1) *Handbook of Oligo- and Polythiophenes*; Wiley-VCH: Weinheim, 1999.
(2) Janssen, R. A. J.; Smilowitz, L.; Saricifici, N. S.; Moses, D. *J. Chem. Phys.* **1994**, *101*, 1787−1798.
(3) Schneider, M.; Brinkmann, M.; Muccini, M.; Biscarini, F.; Taliani, C.; Gebauer, W.; Sokolowski, M.; Umbach, E. *Chem. Phys.* **2002**, *285*, 345−353.
(4) Marks, R. N.; Muccini, M.; Lunedi, E.; Michel, R. H.; Murgia, M.; Zamboni, R.; Taliani, C.; Horowitz, G.; Garnier, F.; Hopmeier, M.; Oestreich, M.; Mahrt, R. F. *Chem. Phys.* **1998**, *227*, 49−56.
(5) Iannotta, S.; Toccoli, T.; Boschetti, A.; Scardi, P. *Synth. Met.* **2001**, *122*, 221−223.
(6) Kouki, F.; Spearman, P.; Horowitz, G.; Delannoy, P.; Valat, P.; Wintgens, V.; Garnier, F. *Synth. Met.* **1999**, *102*, 1071−1072.
(7) Oelkrug, D.; Egelhaaf, H.-J.; Gierschner, J.; Tompert, A. *Synth. Met.* **1996**, *76*, 249−253.
(8) Hopmeier, M.; Marks, R. N.; Michel, R. H.; Muccini, M.; Murgia, M.; Zamboni, R.; Taliani, C.; Horowitz, G.; Garnier, F.; Oestreich, M.; Mahrt, R. F. *J. Lumin.* **1998**, *76&77*, 416−419.
(9) Yang, A.; Kuroda, M.; Shiraishi, Y.; Kobayashi, T. *J. Chem. Phys.* **1998**, *109*, 8442−8450.
(10) Yang, A.; Kuroda, M.; Shiraishi, Y.; Kobayashi, T. *J. Phys. Chem. B* **1998**, *102*, 3706−3711.
(11) Kanemitsu, Y.; Shimiziu, N.; Suzuki, K.; Shiraishi, Y.; Kuroda, M. *Phys. Rev. B* **1996**, *54*, 2198−2204.

(12) Sassella, A.; Tubino, R.; Borghesi, A.; Botta, C.; Destri, S.; Porzio, W.; Barbarella, G. *Synth. Met.* **1999**, *101*, 538−541.
(13) Tavazzi, S.; Besana, D.; Borghesi, A.; Meinardi, F.; Sassella, A.; Tubino, R. *Phys. Rev. B* **2002**, *65*, 205403-1−205403-7.
(14) Engelhaaf, H.-J.; Oelkrug, D.; Gebauer, W.; Sokolowski, M.; Umbach, E.; Fischer, Th.; Bäuerle, P. *Opt. Mater.* **1998**, *9*, 59−64.
(15) Egelhaaf, H.-J.; Gierschner, J.; Oelkrug, D. *Synth. Met.* **2002**, *127*, 221−227.
(16) O'Regan, B.; Grätzel, M. *Nature (London)* **1991**, *353*, 737−740.
(17) Nazeerudddin, M.-K.; Kay, A.; Rodicio, I.; Humphry-Baker, R.; Müller, E.; Liska, P.; Vlachopoulos, N.; Grätzel, M. *J. Am. Chem. Soc.* **1993**, *115*, 6328.
(18) Kaiser, I.; Ernst, K.; Fischer, C.-H.; Könenkamp, R.; Rost, C.; Sieber, I.; Lux-Steiner, M. Ch. *Sol. Energy Mater. Sol. Cells* **2001**, *67*, 89−96.
(19) O'Regan, B.; Lenzmann, F.; Muis, R.; Wienke, J. *Chem. Mater.* **2002**, *14*, 5023−5029.
(20) O'Regan, B.; Schwartz, D. T.; Zakeeruddin, S. M.; Grätzel, M. *Adv. Mater.* **2000**, *12*, 1263−1267.
(21) Tennakone, K.; Kumara, G. R. R. A.; Wijayantha, K. G. U.; Kottegoda, I. R. M.; Perera, V. P. S.; Aponsu, G. M. L. P. *J. Photochem. Photobiol. A: Chem.* **1997**, *108*, 175−177.
(22) Tennakone, K.; Kumara, G. R. R. A.; Kottegoda, I. R. M.; Perera, V. P. S.; Weerasundara, P. S. R. S. *J. Photochem. Photobiol. A: Chem.* **1998**, *117*, 137−142.
(23) Nanu, M.; Schoonman, J.; Goossens, A. *Adv. Mater.* **2004**, *16*, 453−456.
(24) Brabec, C. J.; Shaheen, S. E.; Fromherz, T.; Padinger, F.; Hummelen, J. C.; Dhanabalan, A.; Janssen, R. A. J.; Saricifci, N. S. *Synth. Met.* **2001**, *121*, 1517−1520.
(25) Brabec, C. J.; Cravino, A.; Meissner, D.; Saricifici, N. S.; Rispens, M. T.; Sanchez, L.; Hummelen, J. C.; Fromherz, T. *Thin Solid Films* **2002**, *403*−*404*, 368−372.
(26) Wienk, M. M.; Kroon, J. M.; Verhees, W. J. H.; Knol, J.; Hummelen, J. C.; van Hal, P. A.; Janssen, R. A. J. *Angew. Chem., Int. Ed.* **2003**, *42*, 3371−3375.
(27) Huynh, W. U.; Dittmer, J. J.; Alivisatos, A. P. *Science* **2002**, *295*, 2425−2427.
(28) Mena-Osteritz, E. *Adv. Mater.* **2002**, *14*, 609−616.
(29) Huisman, C. L.; Goosens, A.; Schoonman, J. *Chem. Mater.* **2003**, *15*, 4617−4624.
(30) van Hal, P. A.; Wienk, M. M.; Kroon, J. M.; Verhees, W. J. H.; Slooff, L. H.; van Gennip, W. J. H.; Jonkheijm, P.; Janssen, R. A. J. *Adv. Mater.* **2003**, *15*, 118−121.
(31) Arango, A. C.; Carter, S. A.; Brock, P. J. *Appl. Phys. Lett.* **1999**, *74*, 1698−1700.
(32) Coakley, K. M.; Liu, Y.; McGehee, M. D.; Frindell, K. L.; Stucky, G. D. *Adv. Mater.* **2003**, *13*, 301−306.
(33) Iarossi, D.; Mucci, A.; Schenetti, L.; Seeber, R.; Goldoni, F.; Affronte, M.; Nava, F. *Macromolecules* **1999**, *32*, 1390−1397.
(34) Hoffman, K. J.; Bakken, E.; Samuelsen, E. J.; Carlsen, P. H. J. *Synth. Met.* **2000**, *113*, 39−44.
(35) Ng, S. C.; Chan, H. S. O.; Miao, P.; Tan, K. L. *Synth. Met.* **1997**, *90*, 25−30.
(36) Pomerantz, M.; Lixin Liu, M. *Synth. Met.* **1999**, *101*, 95.
(37) Murray, K. A.; Holmes, A. B.; Moratti, S. C.; Friend, R. H. *Synth. Met.* **1996**, *76*, 161−163.
(38) Greve, D. R.; Apperloo, J. J.; Janssen, R. A. J. *Synth. Met.* **2001**, *119*, 369−370.
(39) Wu, X.; Chen, T.-A.; Riek, R. D. *Macromolecules* **1996**, *29*, 7671−7677.
(40) Engelmann, G.; Jugelt, W.; Kossmehl, G.; Welzel, H.-P.; Tschuncky, P.; Heinze, J. *Macromolecules* **1996**, *29*, 3370−3375.
(41) Chung, T.-C.; Kaufman, J. H.; Heeger, A. J.; Wudl, F. *Phys. Rev. B* **1984**, *30*, 702−710.
(42) Iarossi, D.; Mucci, A.; Parenti, F.; Schenetti, L.; Seeber, R.; Zanari, C.; Forni, A.; Tonelli, M. *Chem. Eur. J.* **2001**, *7*, 676−685.
(43) Hernandez, J. E.; Ahn, H.; Whitten, J. E. *J. Phys. Chem. B* **2001**, *105*, 8339−8344.
(44) Raza, H.; Wincott, P. L.; Thornton, G.; Casanova, R.; Rodriguez, A. *Surf. Sci.* **1997**, *390*, 256−260.
(45) Land, T. A.; Hemminger, J. C. *Surf. Sci.* **1992**, *268*, 179−188.
(46) Fujitsuka, M.; Sato, T.; Segawa, H.; Shimidzu, T. *Chem. Lett.* **1995**, 99−100.
(47) Nishio, S.; Okada, S.; Minamimoto, Y.; Okumura, M.; Matsuzaki, A.; Sato, H. *J. Photochem. Photobiol. A: Chem.* **1998**, *116*, 245−249.
(48) Paraguay, F. D.; Estrada, W. L.; Acosta, D. R. N.; Andrade, E. M.; Miki-Yoshida, M. *Thin Solid Films* **1999**, *350*, 192−202.
(49) van der Zanden, B.; Goossens, A.; Schoonman, J. *Synth. Met.* **2001**, *121*, 1601−1602.
(50) Cao, Y.; Yu, G.; Zhang, C.; Menon, R.; Heeger, A. J. *Synth. Met.* **1997**, *87*, 171−174.

MA0357265